3-DIMENSIONAL IMAGING OF PION AND KAON ON THE LIGHT FRONT

—from realistic BS wave function

Chao Shi

Nanjing University of Aeronautics and Astronautics (NUAA)

3-D imaging: GPDs & TMDs

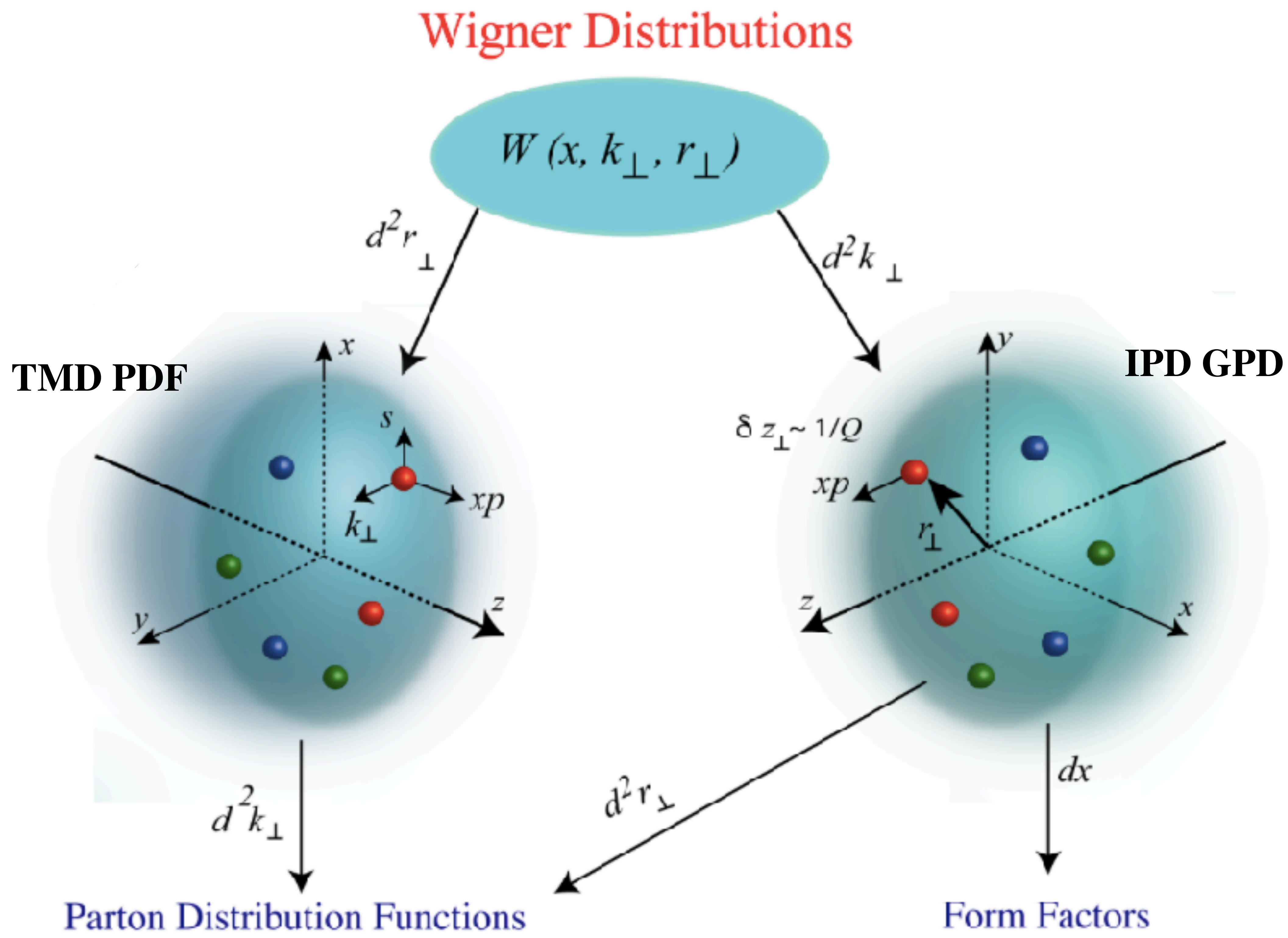

GPDs

1-D correlation function

$$\phi_{ij}(x) = \frac{1}{2}\int \frac{dz^-}{2\pi} e^{ixP^+z^-} \langle P|\bar{\psi}_j(0)\psi_i(z)|P\rangle\Big|_{z^+=z_\perp=0} \longrightarrow [\phi_{ij}\gamma^+] = f(x)$$

GPD correlation function (introducing a momentum transfer)

$$\phi_{ij}(x,\xi,\Delta^2) = \frac{1}{2}\int \frac{dz^-}{2\pi} e^{ixP^+z^-} \left\langle P-\frac{\Delta}{2}\middle|\bar{\psi}_i(0)\psi_j(z)\middle|P+\frac{\Delta}{2}\right\rangle\Big|_{z^+=z_\perp=0}$$

$$\Downarrow$$

$$[\phi_{ij}\gamma^+] = \frac{1}{2P^+}\left[H^q(x,\xi,t)\bar{u}(P+\tfrac{\Delta}{2})\gamma^+u(P-\tfrac{\Delta}{2}) + \ldots\right]$$

GPDs

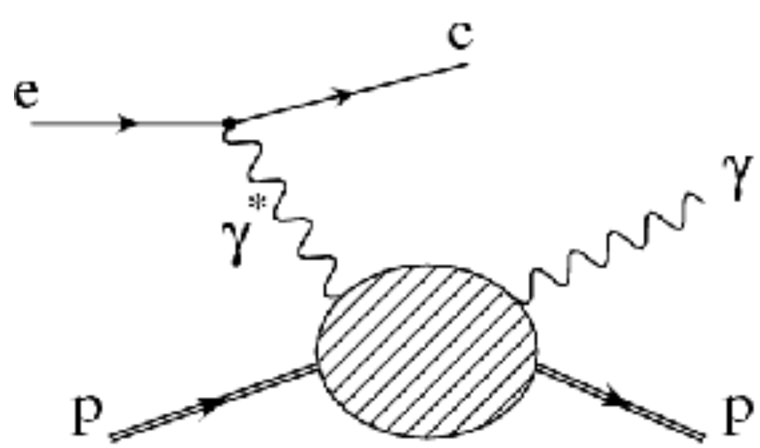

Deeply virtual Compton scattering

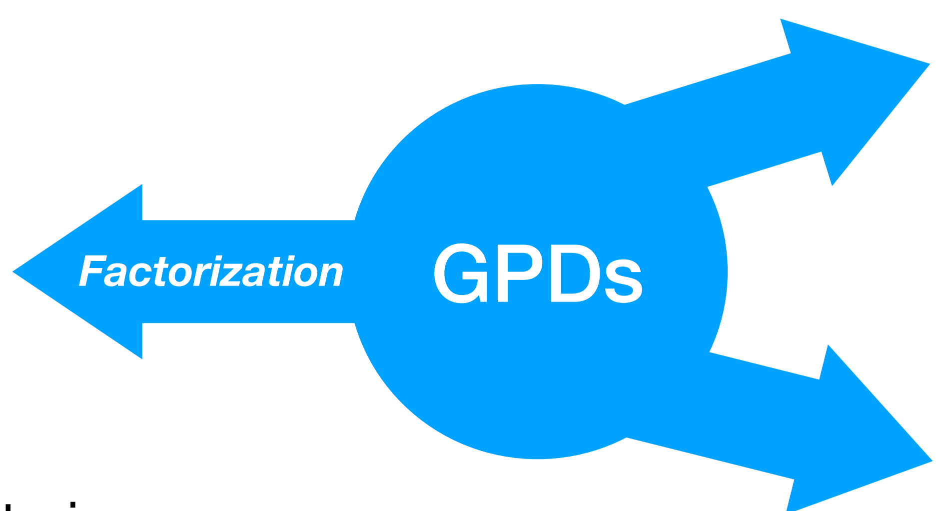

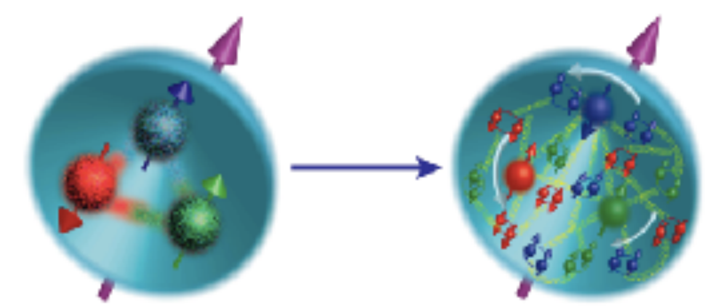

OAM(Ji 1997)

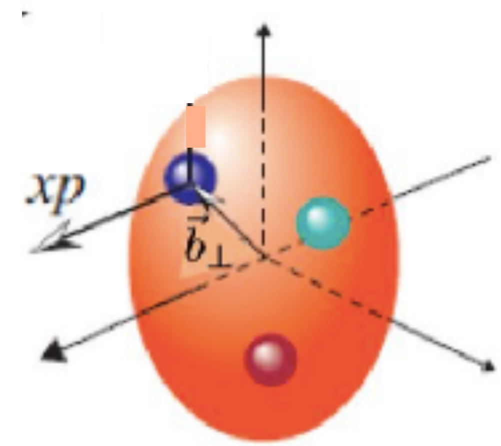

IPD GPD (Burkardt 2000)

TMD PDFs

- The TMD correlation function

$$\Phi_{ij}(x,\boldsymbol{k}_\perp,S) = \int \frac{dz^- d^2\boldsymbol{z}_\perp}{(2\pi)^3} e^{i(k^+ z_- - \boldsymbol{k}_\perp\cdot\boldsymbol{z}_\perp)} \langle P,S|\overline{\psi}_j(0)\psi_i(z)|P,S\rangle\big|_{z^+=0},$$

- The TMD PDFs (leading twist)

$$\begin{aligned}\Phi(x,\boldsymbol{k}_\perp,S) \;=\; & \frac{1}{2}\Big\{ f_1 \not{n}_+ - f_{1T}^\perp \frac{\epsilon_T^{ij} \boldsymbol{k}_\perp^i S_\perp^j}{M} \not{n}_+ + \Lambda g_{1L}\gamma_5 \not{n}_+ + \frac{(\boldsymbol{k}_\perp\cdot\boldsymbol{S}_\perp)}{M} g_{1T}\gamma_5\not{n}_+ + h_{1T}\frac{[\not{S}_\perp,\not{n}_+]}{2}\gamma_5 \\ & + \Lambda h_{1L}^\perp \frac{[\not{k}_\perp,\not{n}_+]}{2M}\gamma_5 + \frac{(\boldsymbol{k}_\perp\cdot\boldsymbol{S}_\perp)}{M} h_{1T}^\perp \frac{[\not{k}_\perp,\not{n}_+]}{2M}\gamma_5 + i h_1^\perp \frac{[\not{k}_\perp,\not{n}_+]}{2M}\Big\},\end{aligned}$$

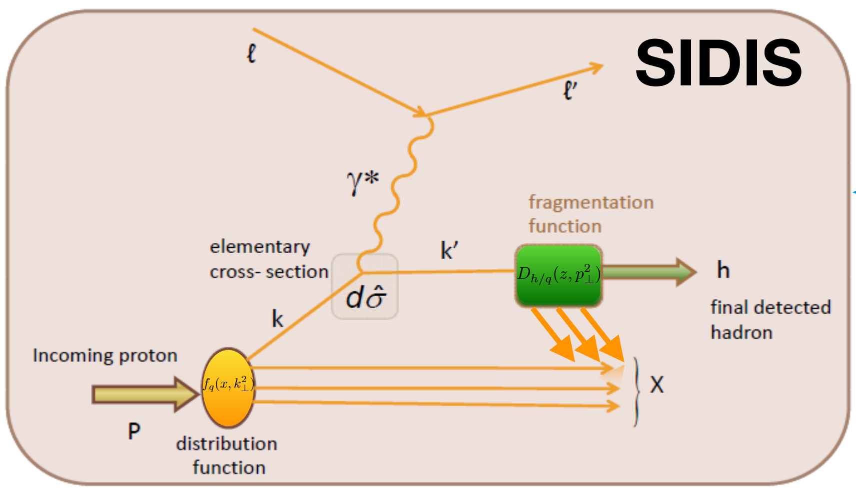

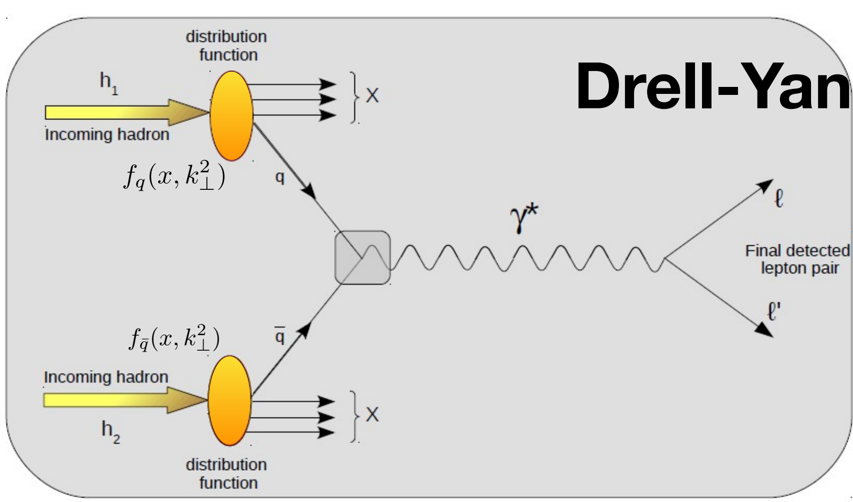

hadron \ quark	*unpolarized*	*chiral*	*transverse*
U	f_1		$h_1^\perp$
L		g_{1L}	$h_{1L}^\perp$
T	$f_{1T}^\perp$	g_{1T}	$h_{1T}, h_{1T}^\perp$

- 3-D momentum distribution and spin-orbit correlations.
- The sign of T-odd Sivers and Boer-Mulders functions are process-dependent. Experimental confirmation is a fundamental test for QCD.

(Collins, PLB 2002)

To obtain GPDs/TMDs: Fit

$d\sigma/dQdq_T$ [nb/GeV^2]

DATA:

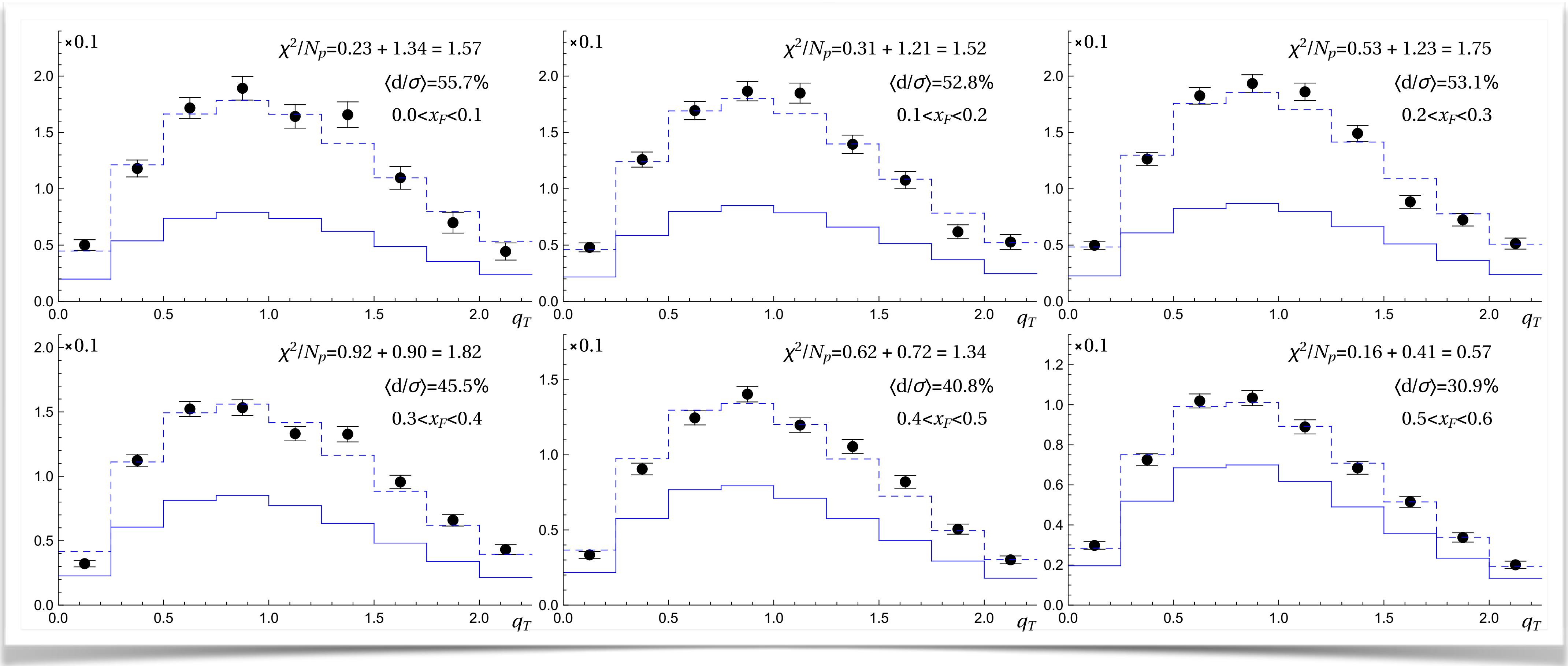

parameterizing & fitting

(Alexey_JHEP2019)

Tomography:

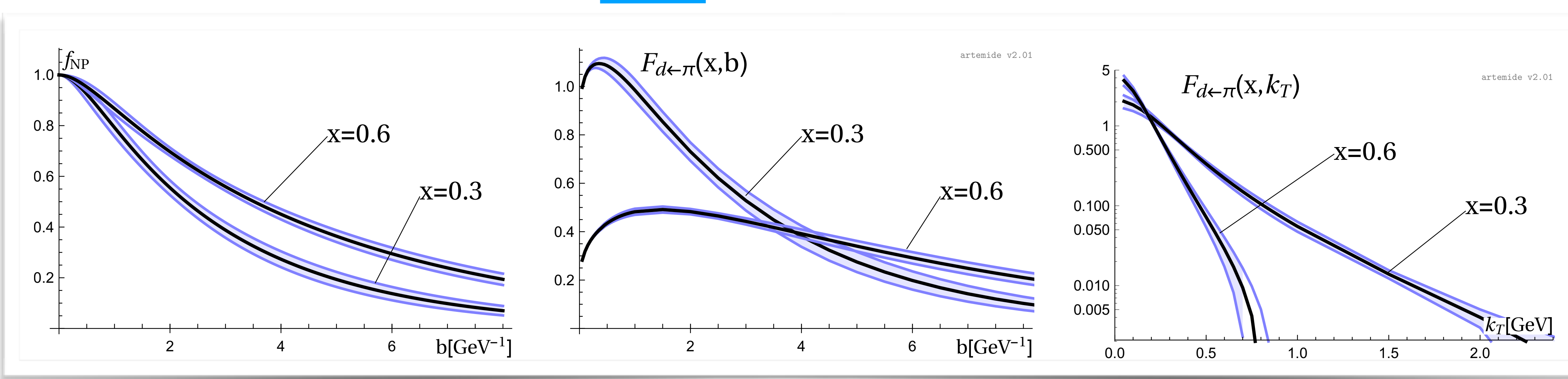

To obtain GPDs/TMDs: Calculation

QCD

$$\mathcal{L}_{\mathrm{QCD}} = \bar{q}_i \gamma^{\mu} (i\partial_{\mu} - g_s t^a A_{\mu}^a - m_i) q_i - \frac{1}{4} F_{\mu\nu}^a F^{a\,\mu\nu}$$

$$F_{\mu\nu}^a = \partial_{\mu} A_{\nu}^a - \partial_{\nu} A_{\mu}^a - g_s f^{abc} A_{\mu}^b A_{\nu}^c \qquad \alpha_s = \frac{g_s^2}{4\pi}$$

Calculation

Nonperturbative QCD methods

1. ADS/QCD
2. Dyson-Schwinger equations.
3. Effective theories and models, e.g., NJL model...
4. Light front QCD.
5. Lattice QCD.

etc...

Transverse momentum dependent distributions (TMD)
3-D tomography in the momentum space.

Generalized parton distributions (GPD)
3-D picture of hadrons in the mixed spatial-momentum space.

A key step to understanding the QCD's non-perturbative properties!

DSE & symmetry preserving

- The Pion&Kaon wave function can be solved by aligning the quark DSE and hadron BSE.

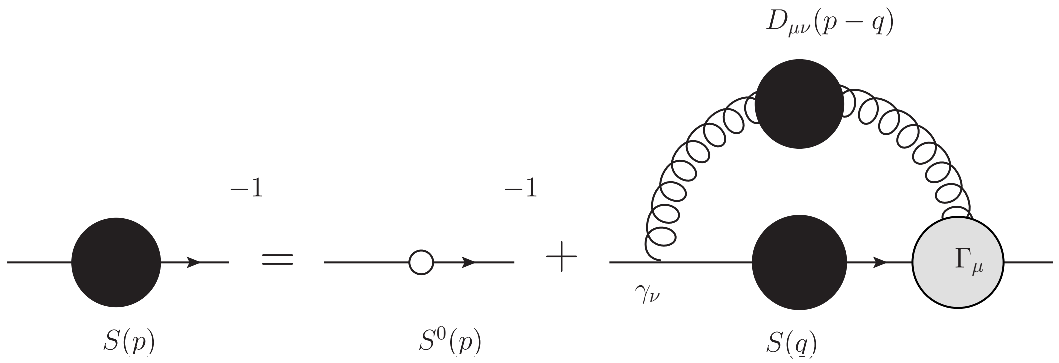

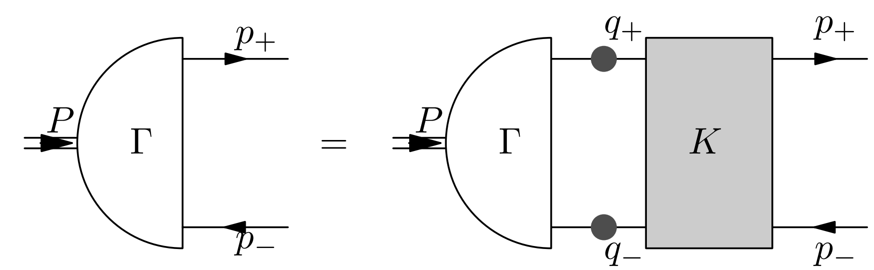

- To solve these equations, truncation is needed for the vertex and scattering kernel. A physically reasonable truncation scheme should respect QCD's (nearly) chiral symmetry, namely, the Axial-Vector Ward-Takahashi Identity

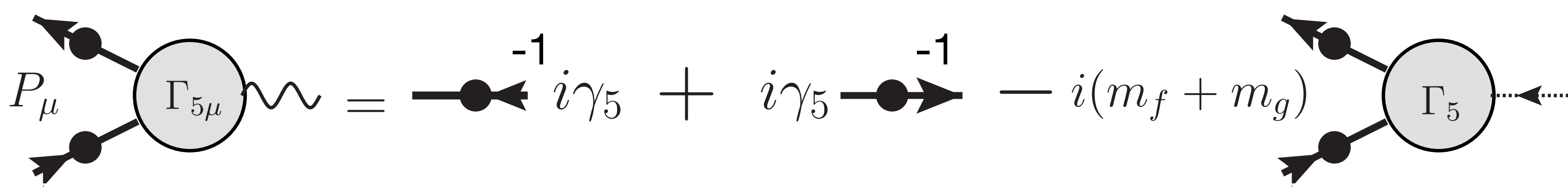

- The simplest manifestation is the Rainbow-Ladder truncation

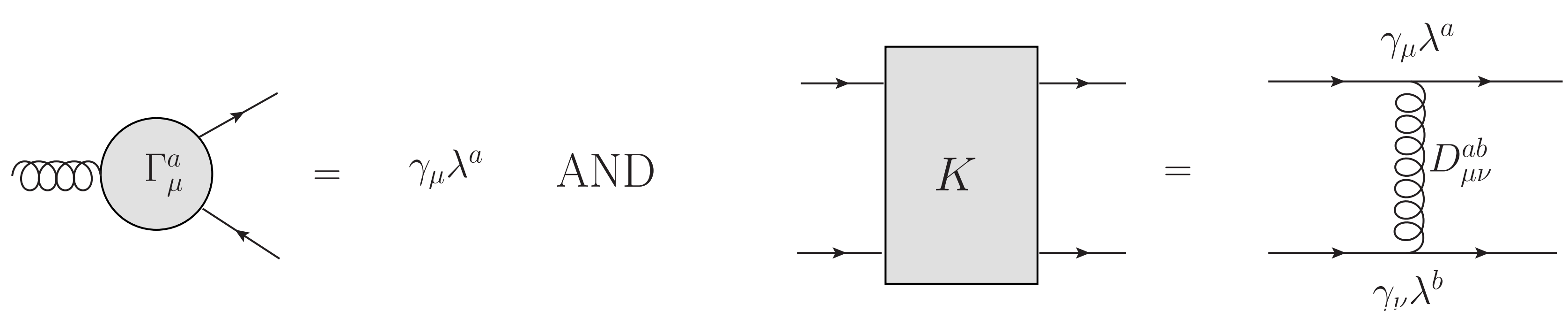

Beyond Rainbow-Ladder

Inhomogeneous BSE

$$\Gamma_{5\mu}(k;P) = Z_2\gamma_5\gamma_\mu$$
$$- Z_2\int_{dq} \mathcal{G}(k-q)\, D^{\rm free}_{\rho\sigma}(k-q)\frac{\lambda^a}{2}\,\gamma_\alpha S(q_+)\times\Gamma_{5\mu}(q;P)S(q_-)\frac{\lambda^a}{2}\,\tilde{\Gamma}_\beta(q_-,k_-)$$
$$+ Z_1\int_{dq} g^2 D_{\alpha\beta}(k-q)\,\frac{\lambda^a}{2}\,\gamma_\alpha S_f(q_+)\times\frac{\lambda^a}{2}\Lambda_{5\mu\beta}(k,q;P)$$

When $P^2 \to -m_\pi^2\,,\ \Gamma^j_{5\mu}(k;P) \sim \dfrac{r_A P_\mu}{P^2+m_\pi^2}\Gamma^j_\pi(k;P)$

(Lei Chang et al, PRL2009)

Beyond-RL kernel

$$\Gamma_\mu(p_1,p_2) = \Gamma^{\rm BC}_\mu(p_1,p_2) + \Gamma^{\rm acm}_\mu(p_1,p_2)$$

$$2\Lambda_{5\beta(\mu)} = [\tilde{\Gamma}_\beta(q_+,k_+)+\gamma_5\tilde{\Gamma}_\beta(q_-,k_-)\gamma_5]\times\frac{1}{S^{-1}(k_+)+S^{-1}(-k_-)}\Gamma_{5(\mu)}(k;P)$$
$$+\Gamma_{5(\mu)}(q;P)\frac{1}{S^{-1}(-q_+)+S^{-1}(q_-)}\times[\gamma_5\tilde{\Gamma}_\beta(q_+,k_+)\gamma_5+\tilde{\Gamma}_\beta(q_-,k_-)]$$

(Lei Chang et al, PRL2011,PRC2012)

Pion & Kaon : motivation

- Pion (and kaon) has the dual roles of being both a QCD bound state and also the Goldstone boson. In the presence of DCSB, one can't fully appreciate the massness of proton without understanding the masslessness of pion.

(Craig Roberts, FBSY 2017)

- Pion (and kaon) can be directly measured through Drell-Yan process.

- Pion (and kaon) plays an important role in baryon in terms of meson cloud. Consequently, it's also measurable through the Sullivan process.

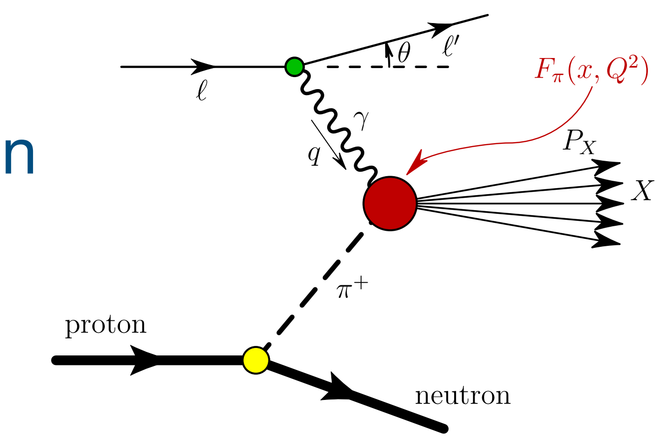

Sullivan process

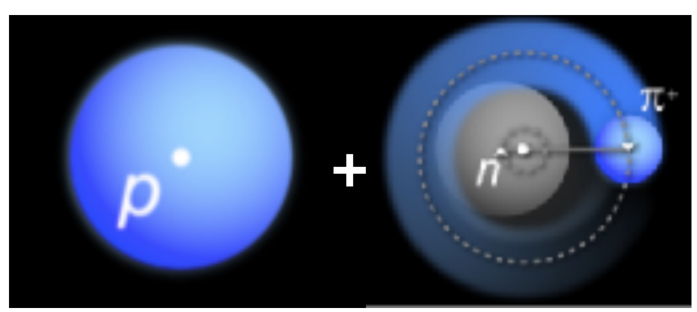

- Theoretically, the study of pion and kaon is well established in DSEs. The TMDs and GPDs pose a new challenge.

TMDs & GPDs: Light-front approach

DSEs:

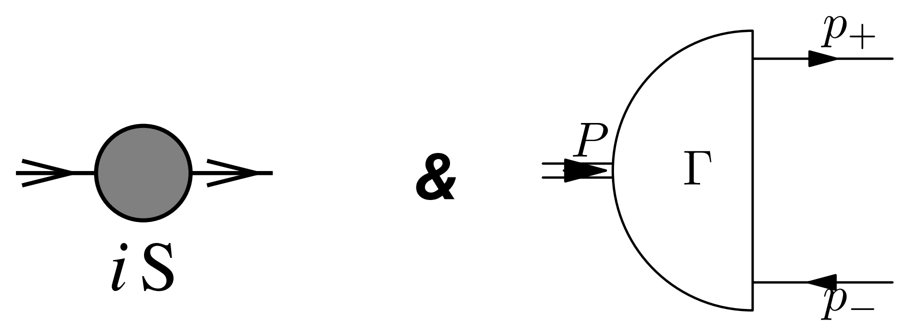

Light front wave functions + overlap representation
(Light front QCD)

TMD & GPD

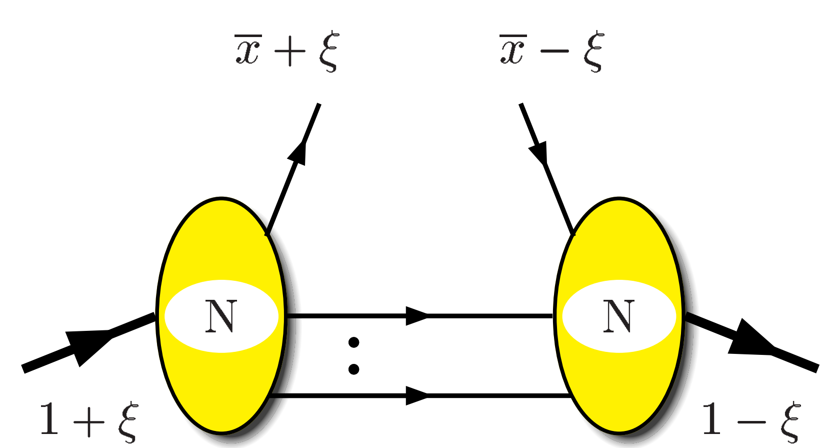

Light-front QCD

- QCD quantized in light front coordinate. A natural formalism in describing hard hadron scattering. The PDF, GPDs and TMDs are all defined on the light front null plane. $\xi^+ = 0$

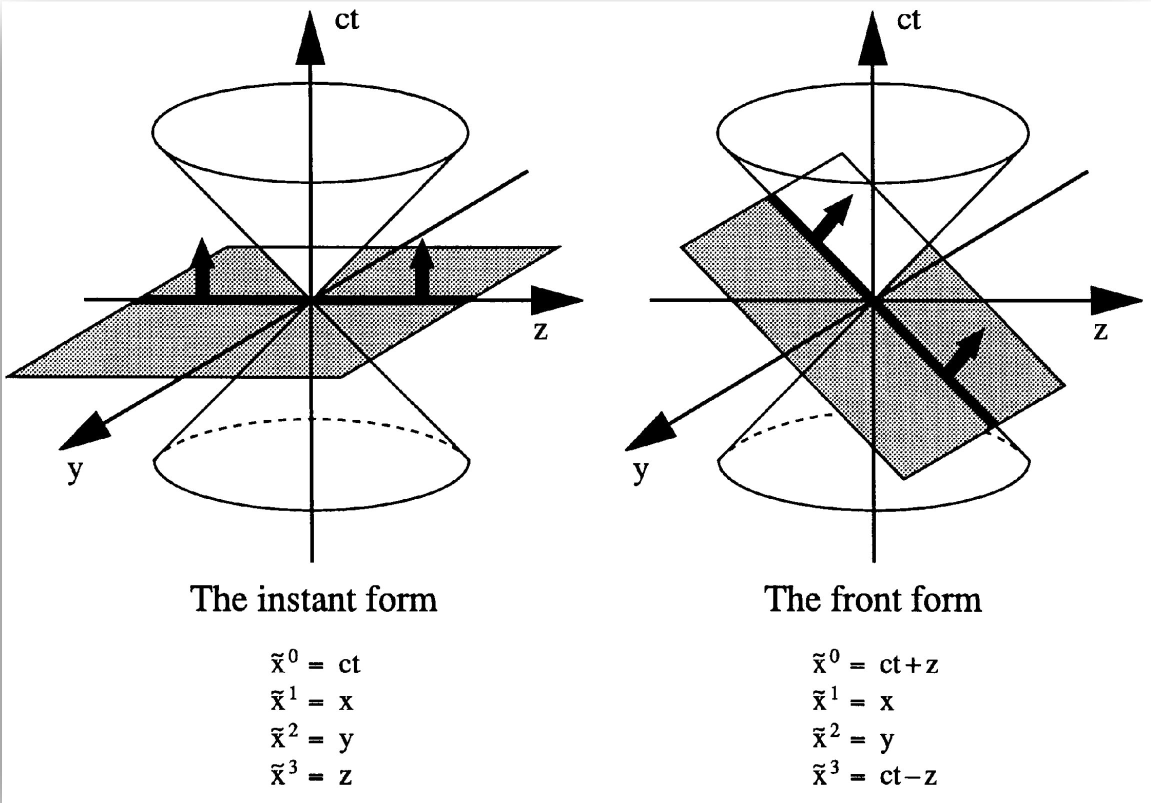

- In the light-front formalism, the hadronic state takes a Fock-state expansion, characterized by light front wave functions.

- The light front wave functions (LFWFs) encode all the non-perturbative dynamical information of the hadron's internal structure.

- To calculate the LFWFs, the standard way is to diagonalize the light-cone Hamiltonian. However, this is very challenging in QCD. In practice, light-cone Hamiltonian models are employed (light-front potential, holographic QCD, NJL model....)

BSE approach

- An alternative way to calculate the LFWFs.

  "...he ('t Hooft) did not use the light–cone formalism and which nowadays might be called standard. Instead, he started from covariant equations... The light–cone Schrodinger equation was then obtained by projecting the Bethe–Salpeter equation onto hyper-surfaces of equal light–cone time. In this way, one avoids to explicitly derive the light–cone Hamiltonian, which, as explained above, can be a tedious enterprise in view of complicated constraints one has to solve..." (Thomas Heinzl)

- BS WFs & LFWFs

$$\langle 0|\bar{d}_+(0)\gamma^+\gamma_5 u_+(\xi^-,\xi_\perp)|\pi^+(P)\rangle = i\sqrt{6}P^+\psi_0(\xi^-,\xi_\perp),$$
$$\langle 0|\bar{d}_+(0)\sigma^{+i}\gamma_5 u_+(\xi^-,\xi_\perp)|\pi^+(P)\rangle = -i\sqrt{6}P^+\partial^i\psi_1(\xi^-,\xi_\perp).$$

(M. Burkardt et al, PLB 2002)

What we do: solve the BS equation first and then project the BS wave functions onto the light front!

- A synergy between Lagrangian formalism and Hamiltonian formalism.

Advantage: In the DSEs, one can selectively sum infinite many diagrams (which potentially incorporates higher Fock states) and conveniently preserves the symmetries of the Lagrangian.

LFWFs & Bethe-Salpeter wave function

Fock state & LFWFs

LFWFs

$$|\pi^+(P)\rangle = |\pi^+(P)\rangle_{l_z=0} + |\pi^+(P)\rangle_{|l_z|=1}$$

$$|\pi^+(P)\rangle_{l_z=0} = i\int \frac{d^2k_\perp}{2(2\pi)^3}\frac{dx}{\sqrt{x\bar{x}}}\psi_0(x,k_\perp^2)\frac{\delta_{ij}}{\sqrt{3}}\frac{1}{\sqrt{2}}[b^\dagger_{u\uparrow i}(x,k_\perp)d^\dagger_{d\downarrow j}(\bar{x},\bar{k}_\perp) - b^\dagger_{u\downarrow i}(x,k_\perp)d^\dagger_{d\uparrow j}(\bar{x},\bar{k}_\perp)]|0\rangle,$$

$$|\pi^+(P)\rangle_{|l_z|=1} = i\int \frac{d^2k_\perp}{2(2\pi)^3}\frac{dx}{\sqrt{x\bar{x}}}\psi_1(x,k_\perp^2)\frac{\delta_{ij}}{\sqrt{3}}\frac{1}{\sqrt{2}}[k_\perp^- b^\dagger_{u\uparrow i}(x,k_\perp)d^\dagger_{d\uparrow j}(\bar{x},\bar{k}_\perp) + k_\perp^+ b^\dagger_{u\downarrow i}(x,k_\perp)d^\dagger_{d\downarrow j}(\bar{x},\bar{k}_\perp)]|0\rangle,$$

LFWFs & BS wave function:

Realistic BS wave function

Project on to the light front
(light front time $\xi^+=0$)

$$\psi_0(x,\boldsymbol{k}_T^2) = \sqrt{3}\,i\int\frac{dk^+dk^-}{2\,\pi}\times \mathrm{Tr}_D\left[\gamma^+\gamma_5\chi(k,p)\right]\delta\left(x\,p^+ - k^+\right),$$

$$\psi_1(x,\boldsymbol{k}_T^2) = -\sqrt{3}\,i\int\frac{dk^+dk^-}{2\,\pi}\frac{1}{\boldsymbol{k}_T^2}\times \mathrm{Tr}_D\left[i\sigma_{+i}\boldsymbol{k}_T^i\,\gamma_5\,\chi(k,p)\right]\delta\left(x\,p^+ - k^+\right),$$

(C. Mezrag et al, FBSY 2016)

LFWFs: $\psi_0(x, k_\perp^2)$ & $\psi_1(x, k_\perp^2)$

- Point-wise accurate LFWFs extracted from parameterized realistic BS wave functions.
- ψ0 (spin-antiparallel) and ψ1 (spin-parallel) is comparable in strength, suggesting the spin parallel contribution also has considerable contribution. Highly relativistic system.
- Strong support at infrared k_T, a consequence of the DCSB which generates significant strength in the infrared region of BS wave function.
- At ultraviolet of k_T, ψ0 scale as $1/k_T^2$ and ψ1 scale as $1/k_T^4$, as has been predicted by pQCD. (one-gluon exchange dominance.)
- SU(3) flavor symmetry breaking effect: u/d and s quark mass difference masked by DCSB.

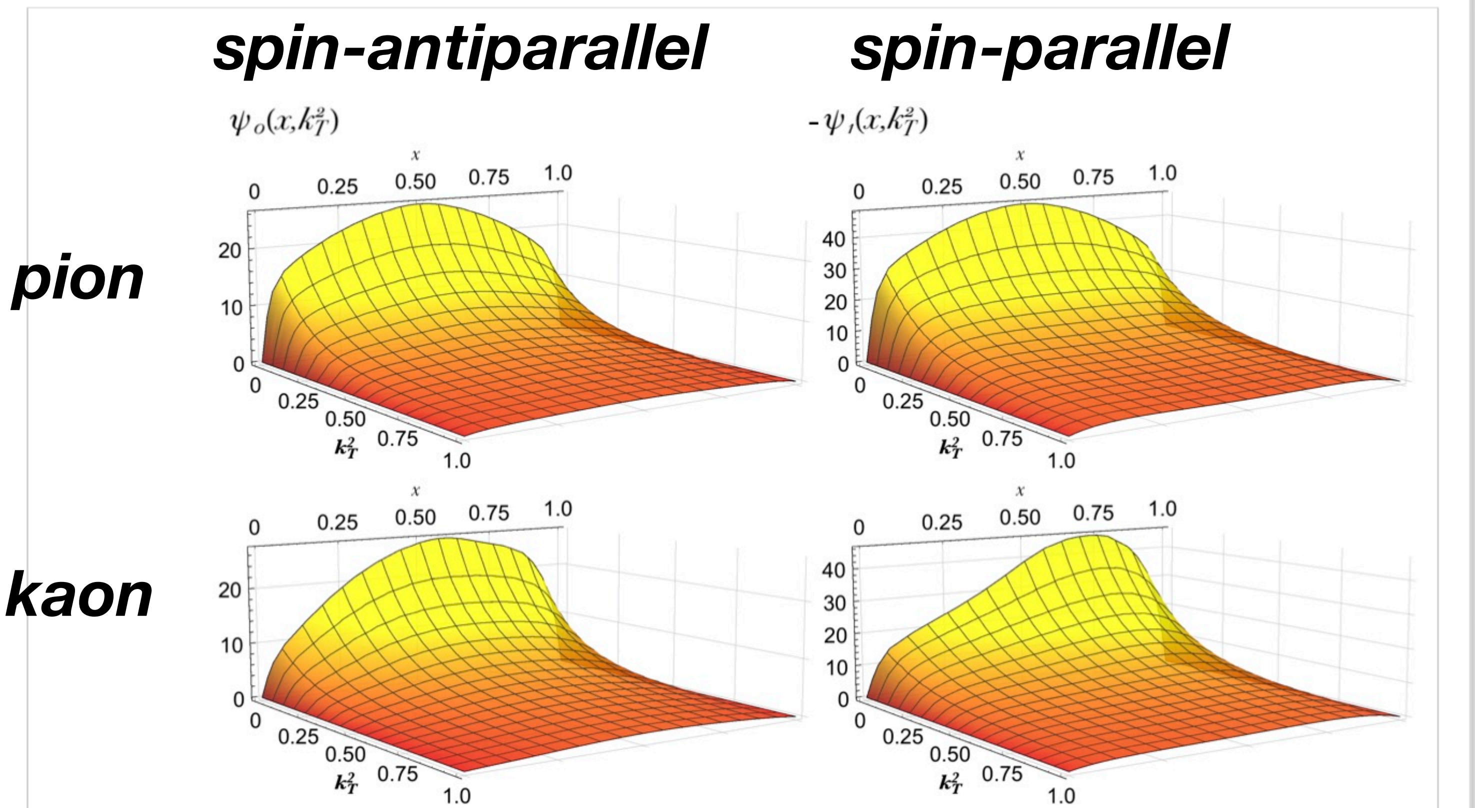

(C.S. et al, arXiv:2003.03037, accepted by PRD)

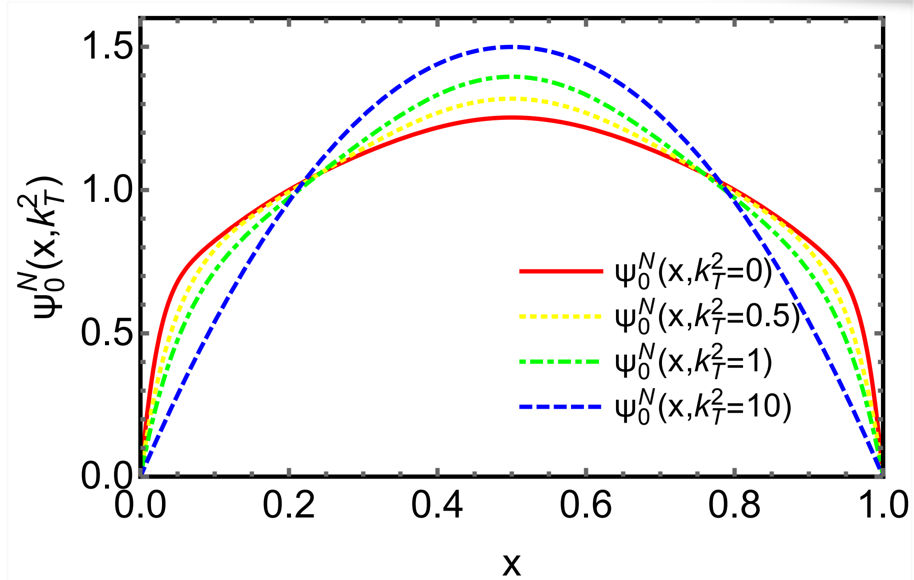

FIG. 2. Pion's spin-anti-parallel LFWF $\psi_0(x, \boldsymbol{k}_T^2)$ at different values of $\boldsymbol{k}_T^2$, normalized to $\psi_0^N(x, \boldsymbol{k}_T^2) = \frac{\psi_0(x,\boldsymbol{k}_T^2)}{\int_0^1 dx \psi_0(x,\boldsymbol{k}_T^2)}$.

GPD overlap representation

- At leading twist, the pion has one GPD:

$$H_{\pi}^{q}(x,\xi,t) = \frac{1}{2}\int \frac{dz^-}{2\pi} e^{ixP^+z^-} \langle p_2|\bar{\psi}^q(-\frac{z}{2})\gamma^+\psi^q(\frac{z}{2})|p_1\rangle|_{z^+=z_\perp=0}$$

- There are two regions, ERBL and DGLAP region, named after their evolution in limiting cases

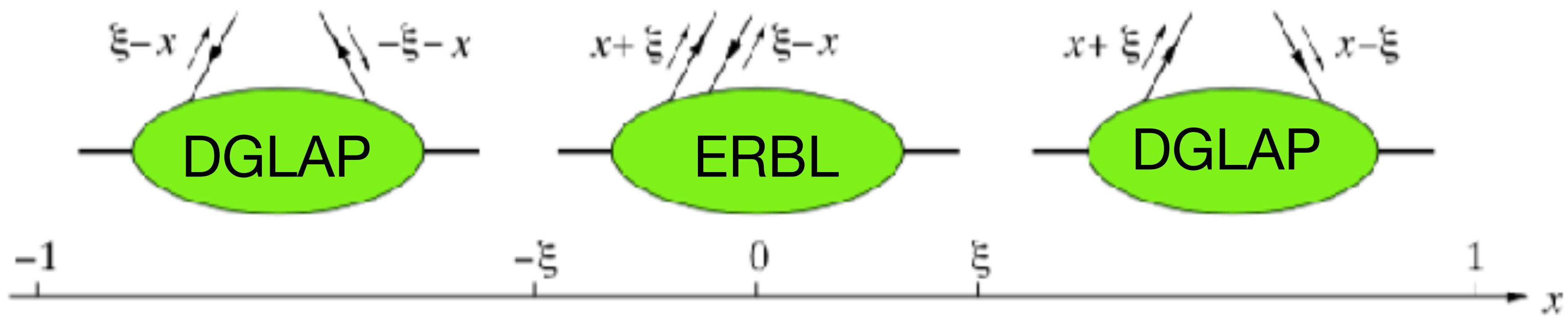

$$\langle\psi_N|\psi_N\rangle \qquad \langle\psi_{N+2}|\psi_N\rangle \qquad \langle\psi_N|\psi_N\rangle$$

- The light front overlap representation requires N-N particle LFWF overlap for DGLAP region and N-N+2 for ERBL region. In the DGLAP region (1>=|x|>=|ξ|):

$$H^u_{\pi^+}(x,\xi,t)\Big|_{\xi\leq x} = \int \frac{\mathrm{d}^2\mathbf{k}_\perp}{16\pi^3}\left[\Psi^*_{l=0}\left(\frac{x-\xi}{1-\xi},\hat{\mathbf{k}}_\perp\right)\Psi_{l=0}\left(\frac{x+\xi}{1+\xi},\tilde{\mathbf{k}}_\perp\right) + \hat{\mathbf{k}}_\perp\cdot\tilde{\mathbf{k}}_\perp\,\Psi^*_{l=1}\left(\frac{x-\xi}{1-\xi},\hat{\mathbf{k}}_\perp\right)\Psi_{l=1}\left(\frac{x+\xi}{1+\xi},\tilde{\mathbf{k}}_\perp\right)\right]$$

GPD at zero skewedness

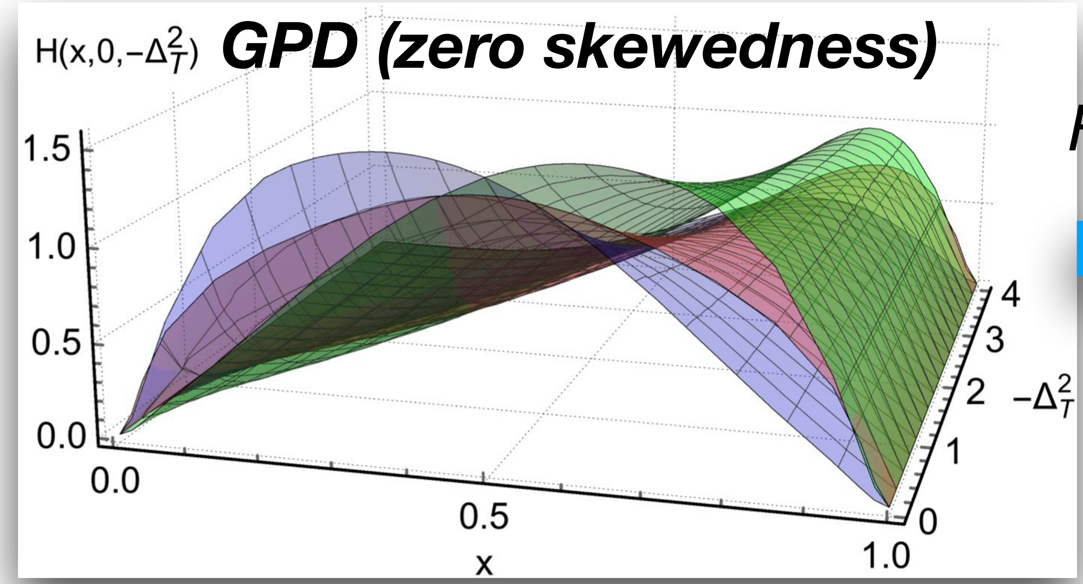

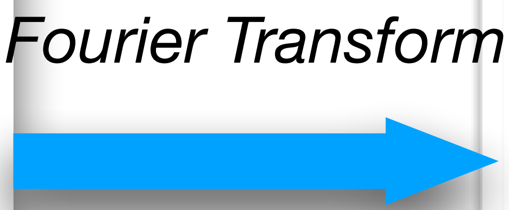

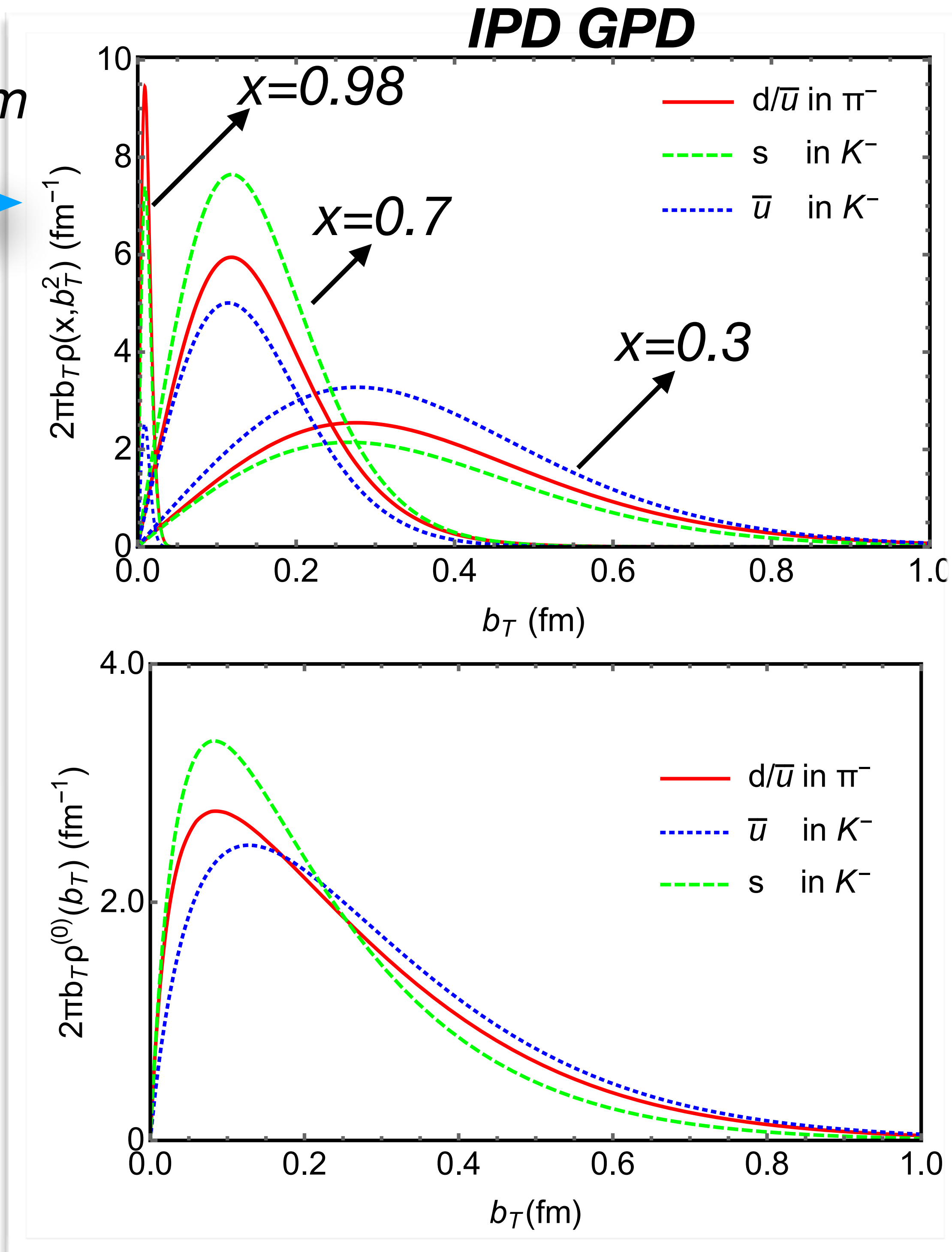

- All distributions peek at the center of impact parameter (note the plot has been multiplied with bT)
- heavier s quark is more localized as compared to light u/d quark, but not too much.

$$\langle b_T^2\rangle = \int d^2b_T b_T^2 \int dx \rho(x, b_T^2)$$

$$\langle b_T^2\rangle_u^\pi = 0.11\mathrm{fm}^2, \langle b_T^2\rangle_s^K = 0.08\mathrm{fm}^2, \langle b_T^2\rangle_u^K = 0.13\mathrm{fm}^2$$

- $\rho^{(0)}(b_T) = \rho_q^{(0)}(b_T) - \rho_{\bar{q}}^{(0)}(b_T)$ is scale-independent, since H(x,0,ΔT) evolution is independent of ΔT.

GPD at zero skewedness

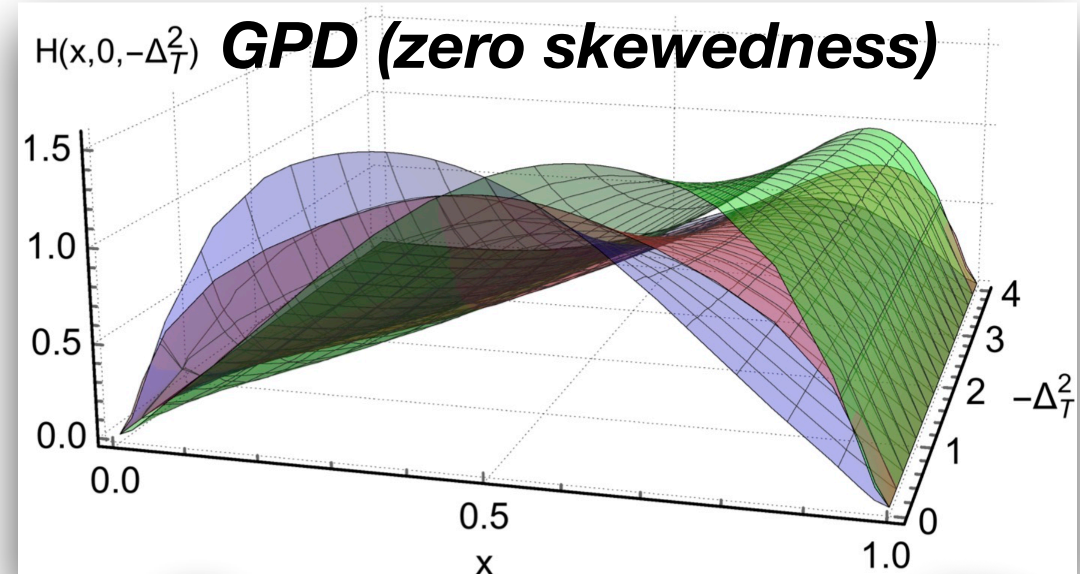

- GFF is in general agreement with lattice simulation.
- EMFF overshoots the data.
- A modification mimicking higher Fock state effect refines EMFF while preserve the GFF simultaneously.

$$\int dx\, x H(x,0,\Delta^2)$$

$$\int dx H(x,0,\Delta^2)$$

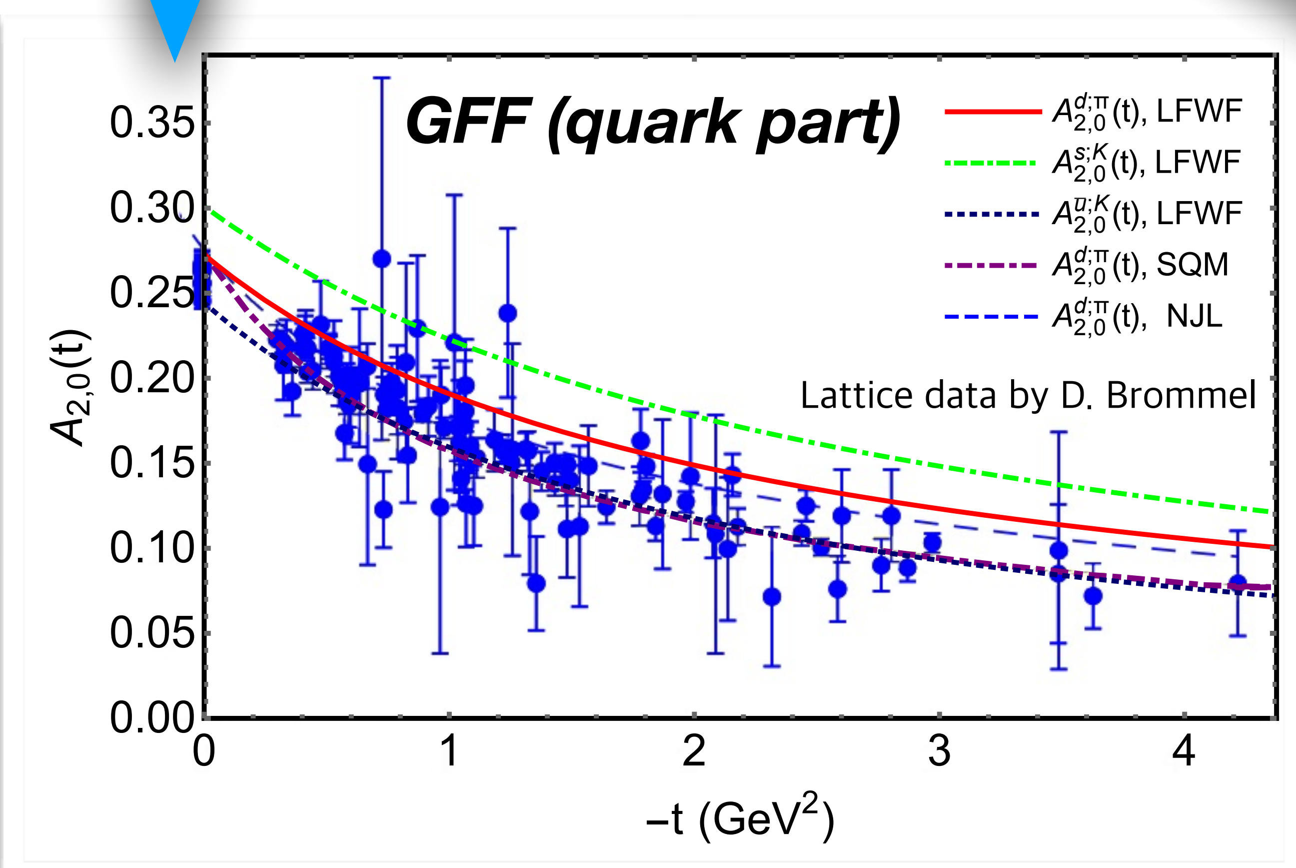

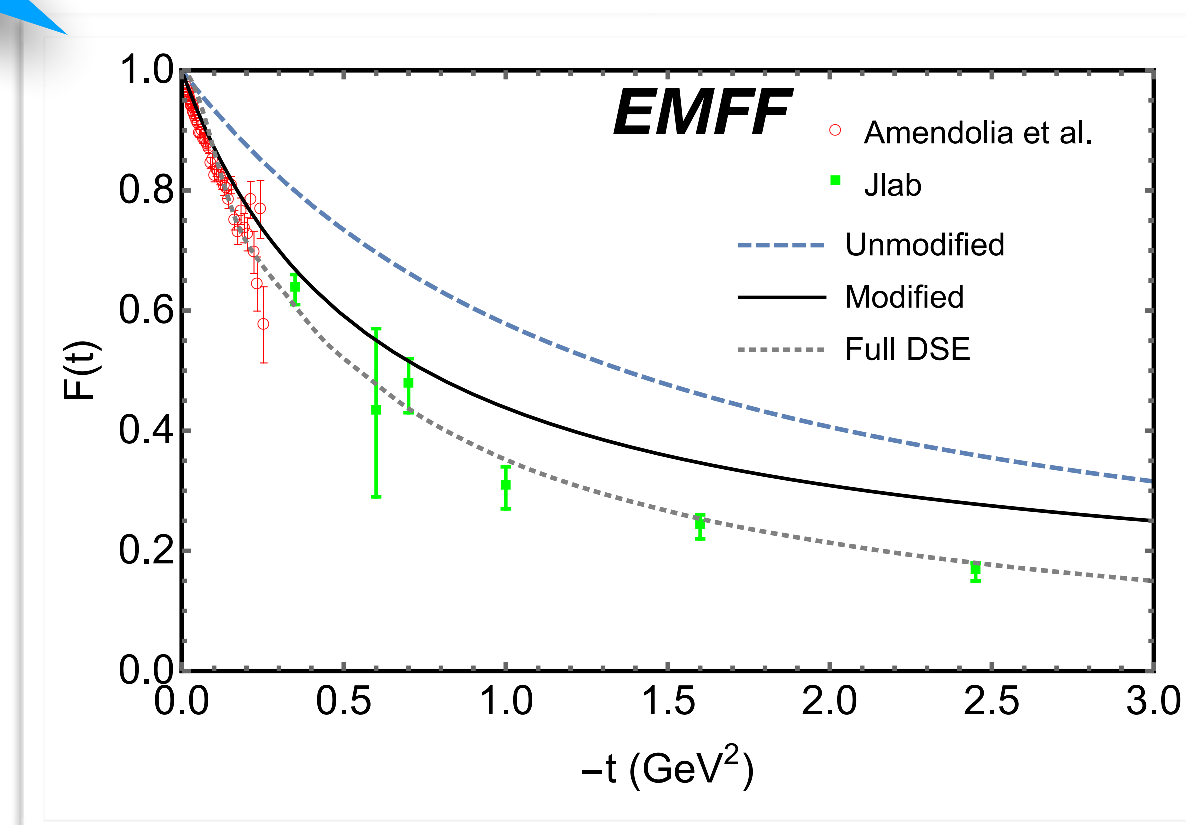

Unpolarized TMD PDF

- TMD overlap representation

$$f_{1,\pi}(x,\mathbf{k}_\perp^2) = |\psi_{\uparrow\downarrow}(x,k_\perp^2)|^2 + k_\perp^2|\psi_{\uparrow\uparrow}(x,k_\perp^2)|^2$$

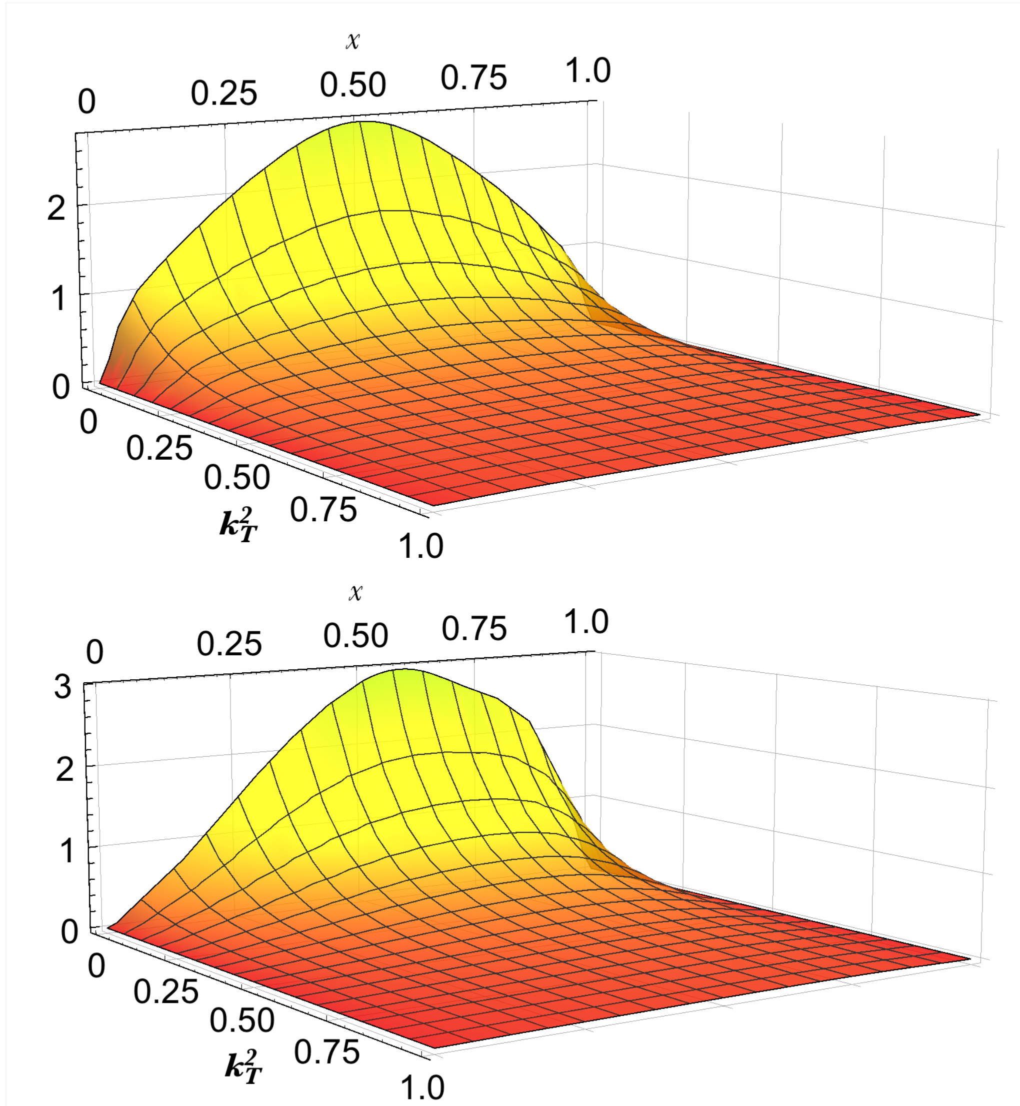

FIG. 7. The unpolarized TMD $f^d_{1;\pi}(x,\boldsymbol{k}_T^2)$ of pion (upper panel) and $f^s_{1;K}(x,\boldsymbol{k}_T^2)$ of kaon (lower panel).

DSE & LF

- Significant strength at low k_T , resembles Gaussian form.
- The TMD of kaon is slightly broader than pion.
- Smooth as compared to holographic QCD.

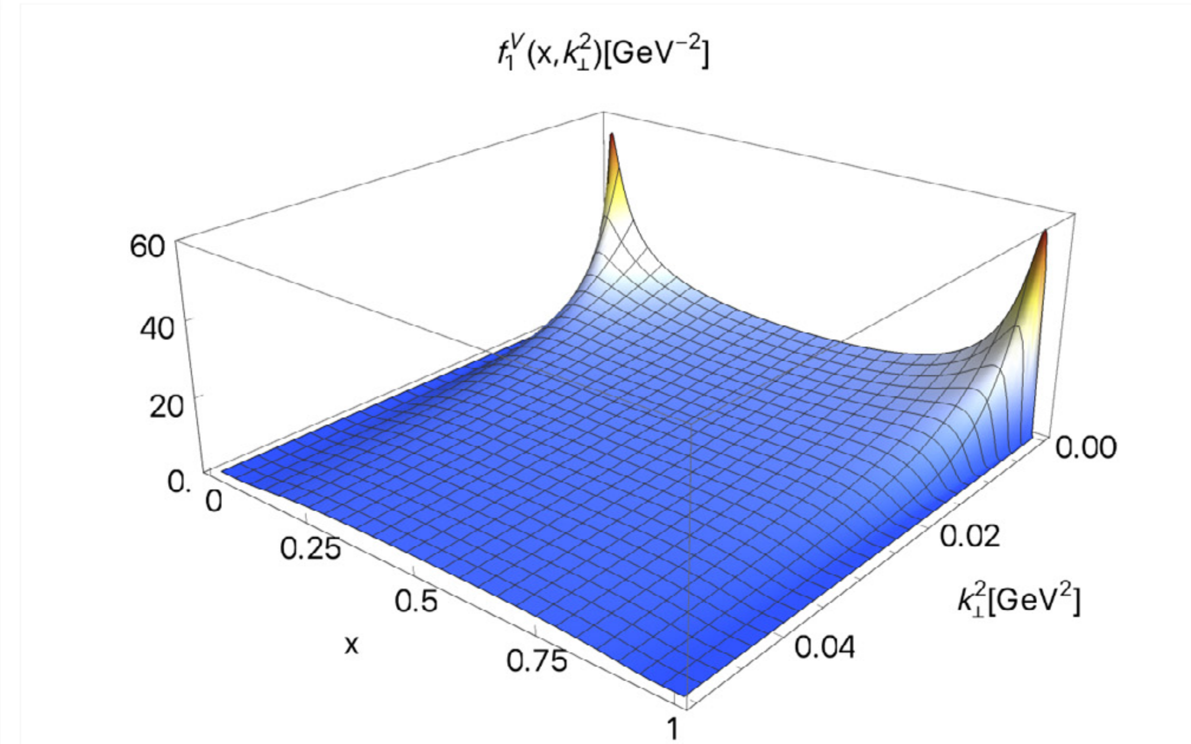

Holographic QCD(A Bacchetta, et al, PLB2017)

TMD evolution

- The TMD evolution is more conveniently worked in coordinate space.

Renormalization group (RG) equation:

$$\mu^2 \frac{d}{d\mu^2} F_{f\leftarrow h}(x,\vec{b};\mu,\zeta) = \frac{1}{2}\gamma_F^f(\mu,\zeta) F_{f\leftarrow h}(x,\vec{b};\mu,\zeta),$$

$$\zeta \frac{d}{d\zeta} F_{f\leftarrow h}(x,\vec{b};\mu,\zeta) = -\mathcal{D}^f(\mu,\vec{b}) F_{f\leftarrow h}(x,\vec{b};\mu,\zeta).$$

Anomalous Dimension

TMD PDF in the coordinate space

The scale μ is the standard RG scale, with the additional rapidity factorization scale ζ to regularize the light-cone divergence arising from Wilson lines. They were usually chosen to be the same order of scattering scale.

Solution:

$$F_{f\leftarrow h}(x,\vec{b};\mu_f,\zeta_f) = \exp\left[\int_P \left(\gamma_F^f(\mu,\zeta)\frac{d\mu}{\mu} - \mathcal{D}^f(\mu,\vec{b})\frac{d\zeta}{\zeta}\right)\right] F_{f\leftarrow h}(x,\vec{b};\mu_i,\zeta_i)$$

TMD evolution:

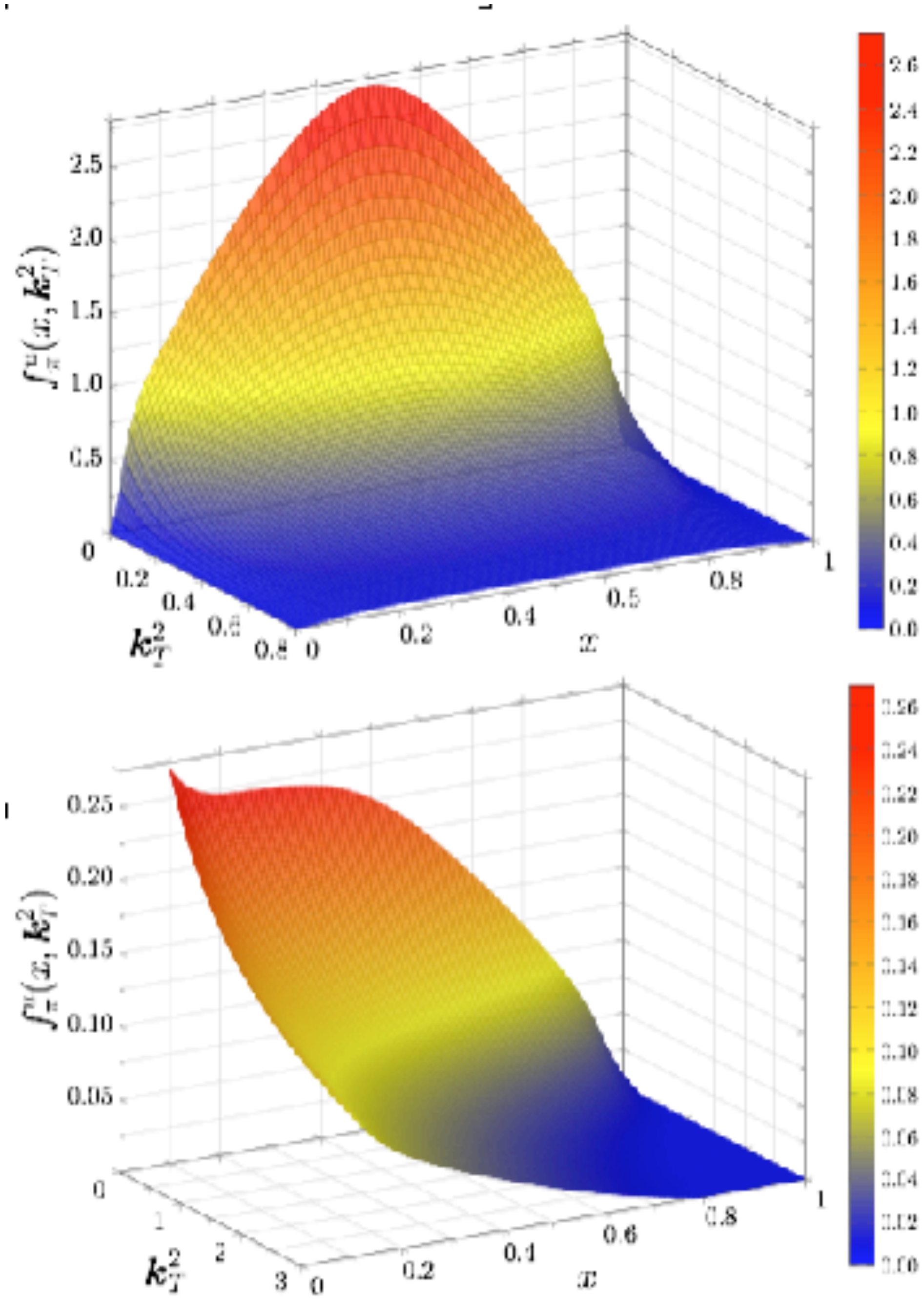

Figure 2. *Upper panel:* DSE result using the DCSB-improved kernel for the time-reversal even u-quark TMD of the pion, $f_\pi^u(x, k_T^2)$, at the model scale of $\mu_0^2 = 0.52\,\mathrm{GeV}^2$. *Lower panel:* Analogous result evolved to a scale of $\mu = 6\,\mathrm{GeV}$ using TMD evolution with the b^* prescription and $g_2 = 0.09\,\mathrm{GeV}$ [43]. The TMDs are given in units of GeV^{-2} and k_T^2 in GeV^2.

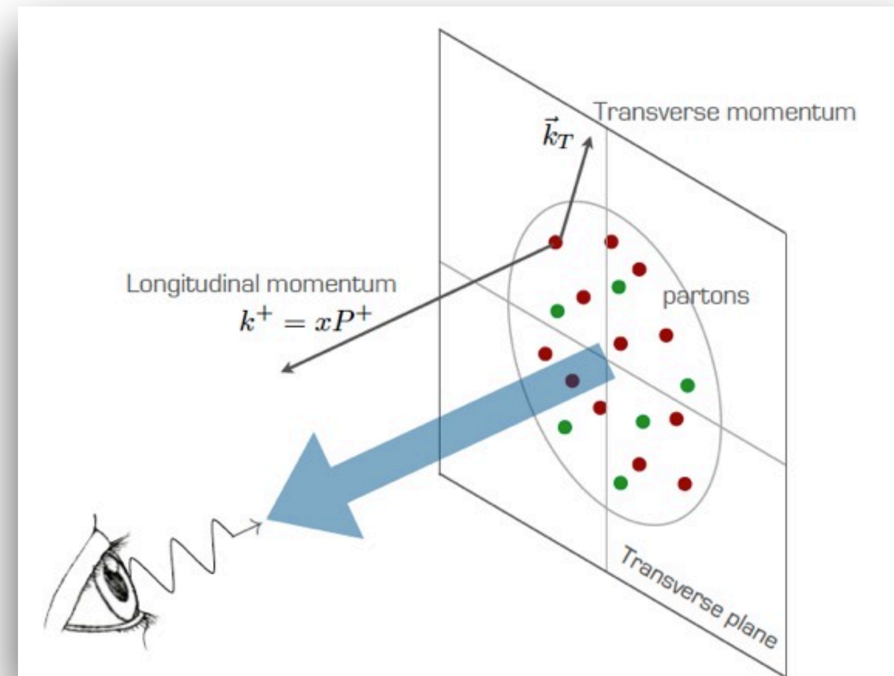

- Evolution has a significant effect, leading to approximately an order of magnitude of suppression at small k_T , and a broad tail at larger k_T.
- The evolved TMD PDF at smaller x is significantly broader than that at large x (Non-factorizable x and k_T dependence).

Drell-Yan Process

Experiment (E615)

Transverse momentum dependence parameterized by function $P(qT;xF ,m\mu\ \mu\ )$

$$\frac{d^3\sigma}{dx_\pi dx_N dq_T} = \frac{d^2\sigma}{dx_\pi dx_N} P(q_T; x_F, m_{\mu\mu}).$$

$$q^0 = \frac{\sqrt{s}}{2}(x_\pi + x_N)$$

$$q^3 = \frac{\sqrt{3}}{2}(x_\pi - x_N)$$

"Experimental study of muon pairs produced by 252-GeV pions on tungsten", Conway, J.S. et al. Phys.Rev. D39 (1989) 92-122.

Theory

$$\frac{d^3\sigma}{dx_\pi dx_N dq_T} \propto |q_T| F^1_{uu}(x_\pi, x_N, q_T)$$

(leading twist)

TMD formalism: $F^1_{UU}(x_1, x_2, q_T) = \frac{1}{N_c}\sum_a e_a^2 \int d^2\boldsymbol{k}_{1\perp} d^2\boldsymbol{k}_{2\perp} \delta^{(2)}(\boldsymbol{q}_T - \boldsymbol{k}_{1\perp} - \boldsymbol{k}_{2\perp}) f^{\bar{a}}_{1,\pi}(x_1, \boldsymbol{k}^2_{1\perp}) f^a_{1,N}(x_2, \boldsymbol{k}^2_{2\perp}).$

offered by DSEs&evolution

borrow from global analysis

Examine: $P(q_T; x_F, m_{\mu\mu}) \propto |q_T| F^1_{UU}(q_T; x_F, \tau)$

E615:

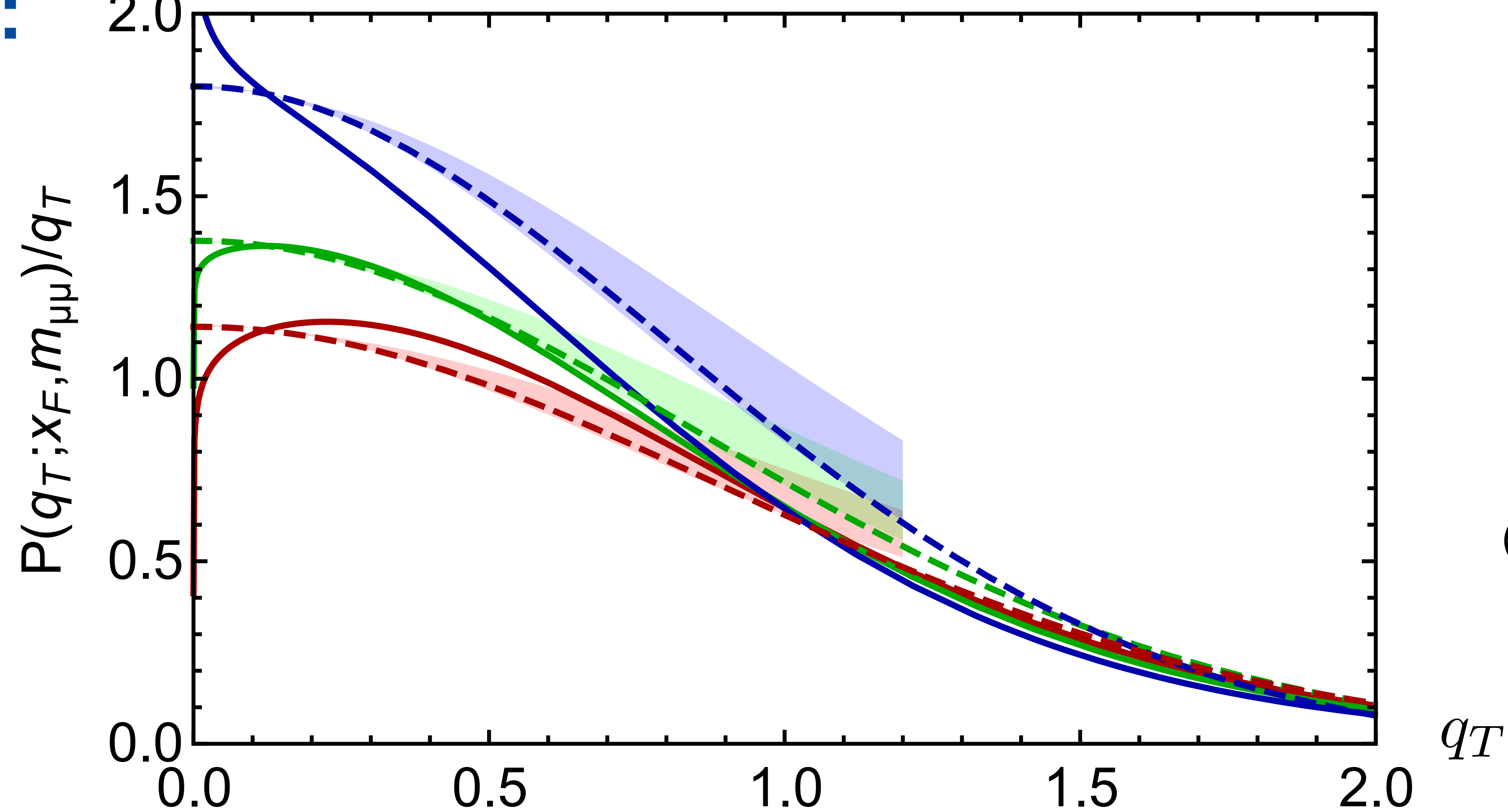

(C.S. et al, PRL2019)

The fitting function $P(q_T; x_F, m_{\mu\mu})/q_T$ at $x_F = 0.0$ (red solid), 0.25 (green solid) and 0.5 (blue solid). The band colored bands are our results based on b*-prescription, with upper boundary corresponding to $g_2 = 0.09$ and lower boundary for $g_0 = 0.0$. The dashed lines are obtained following ζ-prescription where g_2 is found to be consistent with zero at NNLL/NNLO.

- Our results using two evolution schemes generally agree with E615 measurement. In particular, when the non-perturbative sudakov factor goes to zero as suggested by ζ-prescription at higher order. (The deviation is less than 10%for x_F =0 and 0.25, and increases to 30% at most for x_F = 0.5.)
- Our calculation also shows the TMD formalism becomes less valid as x_F goes larger (also in Aurore's talk)

Pion TMD PDF global fit

E615

NLO

b*-pres

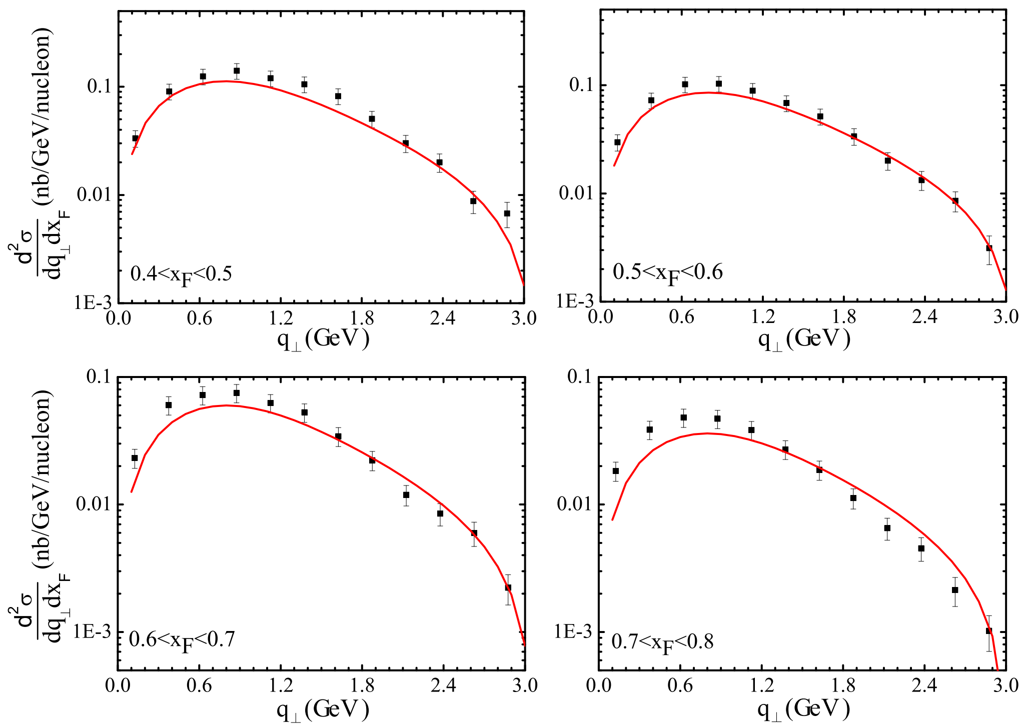

Figure 1. The fitted cross section (solid line) of pion-nucleon Drell-Yan as functions of $q_\perp$, compared with the E615 data (full squre), for different x_F bins in the range $0 < x_F < 0.8$. The error bars shown here include the statistical error and the 16% systematic error.

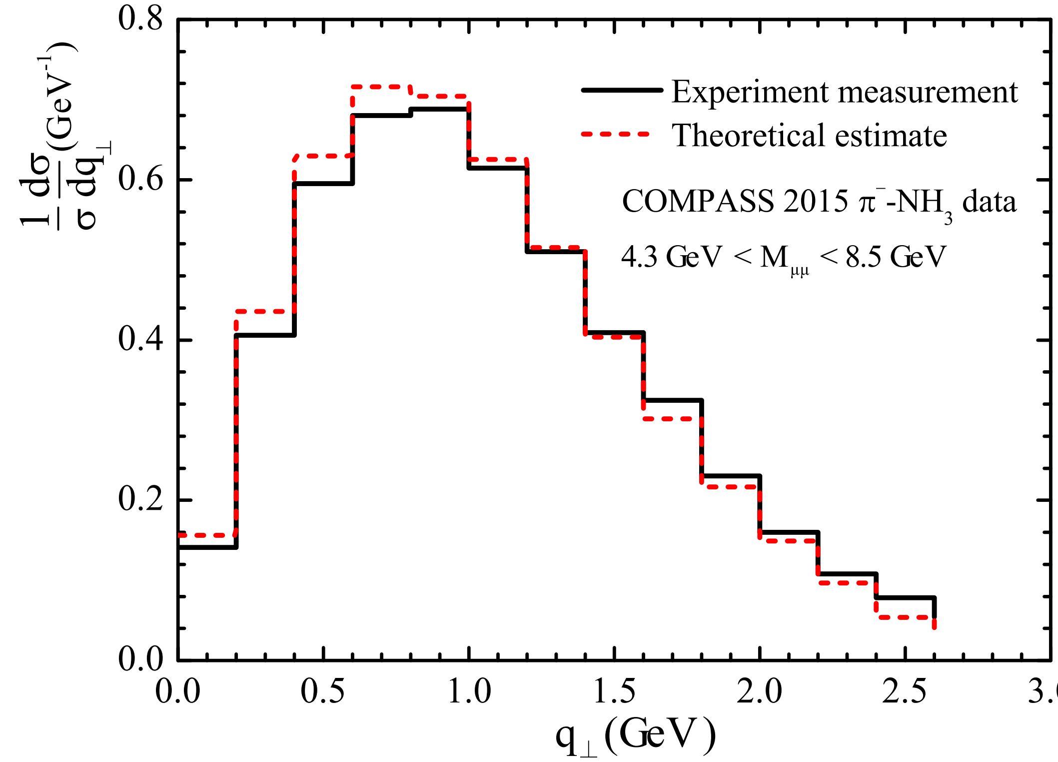

(Xiaoyu, et al, JHEP2017)

Experiment	$\sqrt{s}$ [GeV]	Q [GeV]	x_F	N_{pt}	corr. err.	Typical stat. err.
E537 (Q-diff.)	15.3	$4.0 < Q < 9.0$ in 10 bins	$-0.1 < x_F < 1.0$	60/146	8%	$\sim$ 20%
E537 (x_F-diff.)	15.3	$4.0 < Q < 9.0$	$-0.1 < x_F < 1.0$ in 11 bins	110/165	8%	$\sim$ 20%
E615 (Q-diff.)	21.8	$4.05 < Q < 13.05$ in 10 (8) bins	$0.0 < x_F < 1.0$	51/155	16%	$\sim$ 5%
E615 (x_F-diff.)	21.8	$4.05 < Q < 8.55$	$0.0 < x_F < 1.0$ in 10 bins	90/159	16%	$\sim$ 5%
NA3	16.8, 19.4	$4.1 < Q < 8.5$	$y > 0$ (?)	—	15%	—
	22.9	$4.1 < Q < 4.7$	$0 < y < 0.4$			

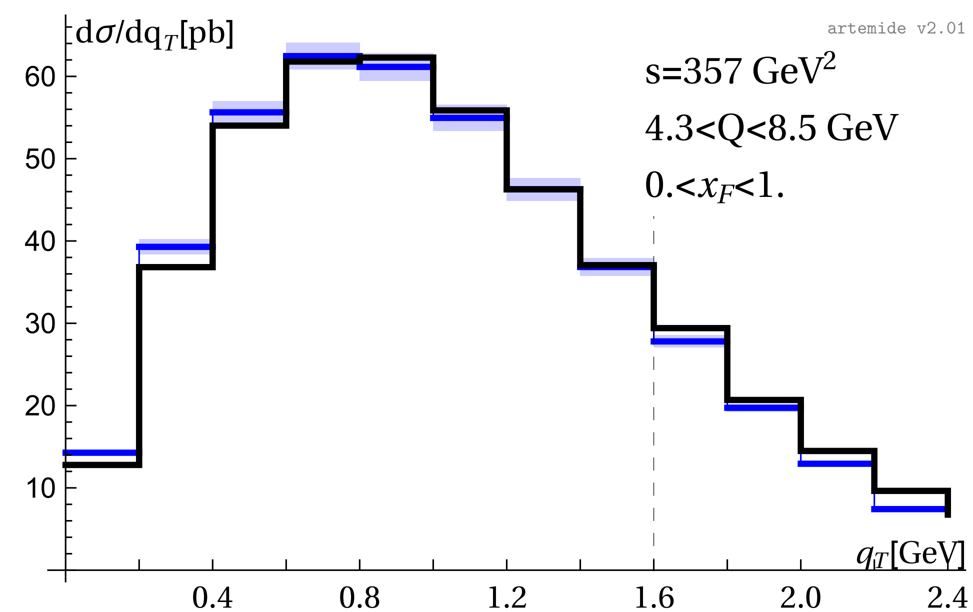

(Alexey Vladimirov, JHEP2019)

NNLO zeta-pres

Normalization problem in E615

Conclusions

- LFWFs can be obtained from Bethe-Salpeter wave functions, rendering a variety of light front distributions calculable.

- In a realistic calculation, the spin-parallel LFWF of pion and kaon contributes considerably, exhibiting a highly relativistic system. How about higher Fock state?

- Higher Fock state appears necessary in a realistic calculation for EMFF. While PDF, GFF and TMD are in general agreement with existing calculations and/or data. Resolved by mimicking higher Fock states.


Thank You